

# Novel Miniature Airflow Energy Harvester for Wireless Sensing Applications in Buildings

Dibin Zhu, Steve P. Beeby, Michael J. Tudor, Neil M. White, *Senior Member, IEEE*, and Nick R. Harris

**Abstract**—This paper presents a novel miniature airflow energy harvester for wireless sensing applications. The energy harvester consists of a wing that is attached to a cantilever spring. The wing oscillates in response to a steady airflow. An electromagnetic transducer is used to extract electrical energy from the airflow-induced oscillations. Both vertical and horizontal orientations are studied. Experiments show that such a generator can operate at airflow speeds as low as  $1.5 \text{ m} \cdot \text{s}^{-1}$ , which compares well to turbines. When the airflow speed is over  $2 \text{ m} \cdot \text{s}^{-1}$ , the average output power exceeds  $90 \text{ } \mu\text{W}$ , which is sufficient for powering wireless sensor nodes in heat, ventilation, and air conditioning systems in buildings.

**Index Terms**—Airflow energy harvesting, electromagnetic, heat, ventilation, and air condition (HVAC), low airflow speed, smart building.

## I. INTRODUCTION

RESEARCH in smart buildings has increased considerably over the last few years [1]. It is the combination of traditional buildings with some intelligent electronic systems, such as security systems, information systems and Heat, Ventilation and Air Condition (HVAC) systems to provide a safe and pleasant working or living environment for building users. One of the most important systems in smart buildings is the HVAC system that provides high quality air to the building users. To achieve this, many sensors, such as temperature, humidity and gas sensors are deployed in air ducts to monitor air quality. There are normally two types of sensors. Wired sensors are powered from the mains power supply but wiring these sensors is costly and time-consuming. The other type is wireless sensors typically powered by batteries. The deployment of wireless sensors is more flexible but batteries have limited energy and need to be replaced from time to time. These battery-powered wireless sensors require maintenance to periodically change the batteries and have to be located in easily accessible locations. Therefore, a better solution is to use energy harvesting techniques to enable self-powered wireless sensors in HVAC systems. Some possible energy sources include thermal energy [2], mechanical energy [3] and

airflow energy [4]. For the HVAC application airflow energy is the most obvious source since it is readily available in air ducts in buildings.

For airflow energy harvesting, the most common and widely used device is a wind turbine [4]. A wind turbine translates airflow into rotational kinetic energy which is then converted into electrical energy via a transducer, typically electromagnetic transducers. Most wind turbine generators are used in large-scale applications that generate kilo- or mega- watts of electric power. There are a few small scale piezoelectric wind turbine generator reported. Holmes and his group reported several MEMS wind turbine electromagnetic generators [5], [6]. Their latest prototype generated up to  $10 \text{ mW}$  at the airflow speed of  $10 \text{ m} \cdot \text{s}^{-1}$ . The reported minimum airflow speed was  $3 \text{ m} \cdot \text{s}^{-1}$  when the generator produced an output power of around  $100 \text{ } \mu\text{W}$  [6]. Priya et al [7] reported a piezoelectric windmill for remote sensing applications. Their device had size of a small desk fan, i.e. a diameter of  $114 \text{ mm}$ , and produced an output power of  $10.2 \text{ mW}$  under normal wind flow when the turbine rotated at a frequency of  $6 \text{ Hz}$ . However, no particular wind speed was mentioned. For wind turbine generators, the efficiency reduces with their volume, due to the increased effect of friction losses in the bearings and the reduced surface area of the blades. Analysis of miniature turbines predicts a power output of  $6 \text{ } \mu\text{W} \cdot \text{cm}^{-2}$  at  $1 \text{ m} \cdot \text{s}^{-1}$  and to achieve  $300 \text{ } \mu\text{W}$  at  $0.5 \text{ m} \cdot \text{s}^{-1}$  would require a rotor diameter of  $22 \text{ cm}$  [8], which is too big for a wireless sensor node, which has a typical volume of a few  $\text{cm}^3$ . Furthermore, rotating components such as bearings suffer from fatigue and wear, especially when miniaturised and are not capable of operating unattended for 25 years [8].

A vibrating airflow energy harvesting device was invented by Humdinger Wind Energy, called a Windbelt generator [9]. The Windbelt generator operates using an aerodynamic phenomenon known as aeroelastic flutter. When a belt is exposed to the airflow at a certain angle, it vibrates in a direction perpendicular to the airflow. With a transducer, electromagnetic in their case, electrical energy can be extracted from the belt's kinetic energy. The micro windbelt generator ( $13 \text{ cm} \times 3 \text{ cm} \times 2.5 \text{ cm}$ ) has an output power over  $2 \text{ mW}$  at airflow speeds higher than  $5.5 \text{ m} \cdot \text{s}^{-1}$  but its output power reduces significantly ( $< 200 \text{ } \mu\text{W}$ ) at low airflow speeds ( $< 3.5 \text{ m} \cdot \text{s}^{-1}$ ). In addition, the windbelt generator can be extremely noisy during operation.

Another novel airflow energy harvesting device is a flapping piezoelectric generator which flaps like a leaf on the tree [10]–[13]. In order for the device to flap in the airflow, the

Manuscript received February 29, 2012; accepted October 22, 2012. Date of publication October 25, 2012; date of current version January 14, 2013. The associate editor coordinating the review of this paper and approving it for publication was Dr. M. R. Yuce.

The authors are with the School of Electronics and Computer Science, University of Southampton, Southampton SO17 1 BJ, U.K. (e-mail: dz@ecs.soton.ac.uk; spb@ecs.soton.ac.uk; mjt@ecs.soton.ac.uk; nmw@ecs.soton.ac.uk; nrh@ecs.soton.ac.uk).

Color versions of one or more of the figures in this paper are available online at <http://ieeexplore.ieee.org>.

Digital Object Identifier 10.1109/JSEN.2012.2226518

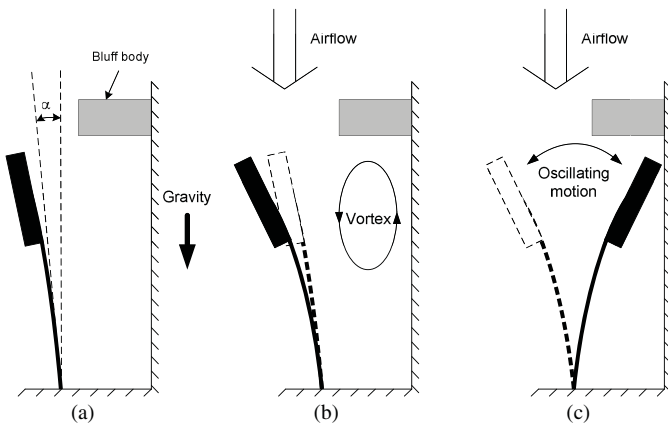


Fig. 1. Operational principle of the flapping generator (vertical orientation). (a) No air flow, initial bending due to the gravity. (b) Cantilever bent due to air flowing. (c) Cantilever sprung back.

structure of the device must be very flexible requiring a very flexible piezoelectric material. Due to the poor piezoelectric strain coefficient of existing flexible materials, the output power of such devices is usually very low. Li et al [10] investigated a flapping airflow energy harvester consisting of a flexible cantilever based on polyvinylidene fluoride or PVDF, a flexible piezoelectric material. Their device produced an output power of  $1.8 \mu\text{W}$  at an airflow speed of  $3.5 \text{ m} \cdot \text{s}^{-1}$ . Ertuk et al [12] reported a flapping airflow generator with an improved flexible piezoelectric material, a Macro Fiber Composite (MFC). An electrical power output of  $10.7 \text{ mW}$  was delivered to a  $100 \text{ k}\Omega$  load at a linear flutter speed of  $9.3 \text{ m} \cdot \text{s}^{-1}$  in their test. However, no airflow speeds were mentioned. Weinstein et al [13] presented a piezoelectric blow energy harvester based on vortex shedding. Power generated by the harvester is between  $100$  and  $3000 \mu\text{W}$  for flow speeds in the range of  $2$  to  $5 \text{ m} \cdot \text{s}^{-1}$ .

In this paper, a type of novel cantilever-based electromagnetic flapping airflow generator is reported. Its operation principle is presented first followed by design and optimization of the generator. Devices with both vertical and horizontal orientation were investigated. Finally, the test results are presented and discussed.

## II. BASICS

### A. Principles

The flapping airflow generator presented here is based on oscillations of a cantilever facing the direction of the airflow. A wing is attached to the free end of a cantilever spring while the other end of the cantilever is clamped and the cantilever may be placed in either a vertical or horizontal orientation. For the device with vertical orientation, as shown in Fig. 1(a), there is an initial downward displacement of the wing due to gravity. The air flowing through the wing causes the cantilever to bend as shown in Fig. 1(b), the degree of bending being a function of the lift/drag force from the wing and the spring constant. Under normal conditions this is a static deflection, but this can become dynamic by causing the lift force to be asymmetric above and below the wing. This is achieved by placing a bluff body, which produces vortices, below the cantilever.

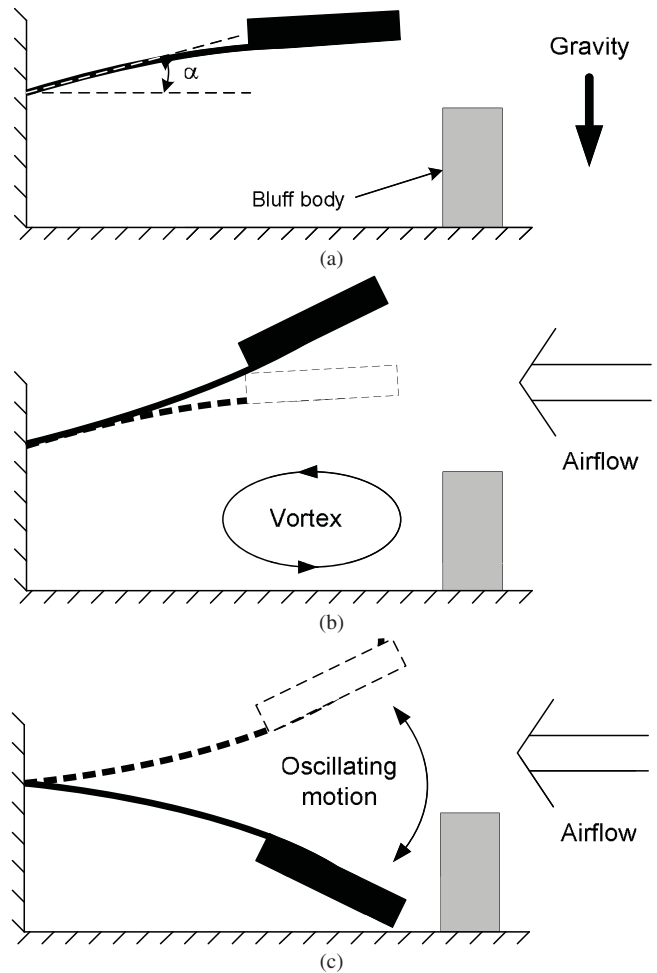


Fig. 2. Operational principle of the flapping generator (horizontal orientation). (a) No air flow, initial downward bending due to the gravity. (b) Cantilever bent due to air flowing. (c) Cantilever sprung back.

As the cantilever deflects, the bluff body reduces the flow of air behind it and the thus lift force reduces, hence causing the cantilever to operate primarily under inertial effects and so spring back as shown in Fig. 1(c). When the cantilever springs back to the initial position, the wing is exposed to the full airflow again, energy is once again extracted from the airflow, and the cycle is repeated. By appropriate design and positioning of the bluff body, and by tuning the resonant frequency of the cantilever spring, the system resonates.

Fig. 2 shows the operational principle of the device in the horizontal orientation. It is similar to that of the device with vertical orientation. The only difference is the role of gravity. In the vertical orientation, gravity helps to start the oscillation as the initial bending is towards the direction where the airflow pushes the wing making it easier to start the oscillation. However, if the airflow is too strong, the airflow together with the gravity may keep the wing at a particular position where it cannot spring back. In the horizontal orientation, the bending due to gravity is in the opposite direction to where the airflow pushes the wing, which makes it more difficult to start the oscillation. Therefore, the wing for the horizontal orientation must be well designed to help the wing oscillate. Once the oscillation starts, gravity will help the

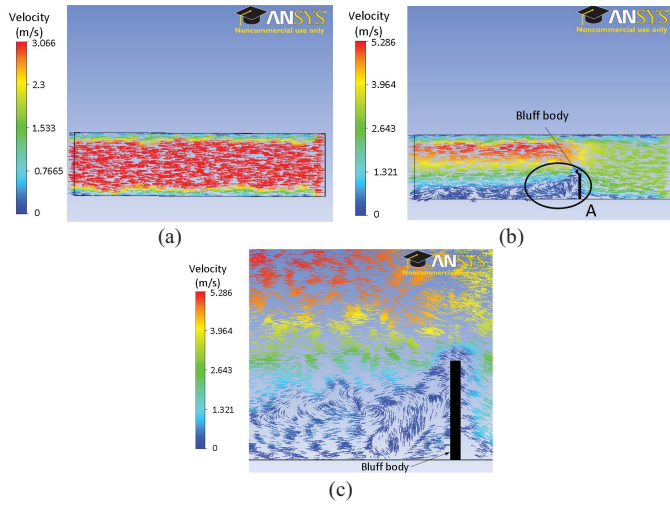


Fig. 3. Comparisons of airflow with and without a bluff body. (a) Airflow without a bluff body. (b) Airflow with a bluff body. (c) Air flow near the bluff body [zoomed-in view of circle A in (b)].

oscillation to sustain. Furthermore, if the airflow becomes strong, gravity can pull the wing downwards to prevent it from stalling.

To assess the effect of the bluff body, simulation was conducted in ANSYS CFX. Fig. 3(a) shows a laminar airflow from right to left without any obstacle in a wind tunnel. The air flow is laminar all the way to the outlet. In fig. 3(b), a bluff body is placed in the wind tunnel. It was found that the airflow over the bluff body remained laminar as its speed increased. In the area behind the bluff body, some vortices were created and airflow speed was significantly reduced. These two outcomes are the key reasons behind the wing generator’s operation.

*B. Measurement of Airflow Speed in the Duct*

Airflow speed in the duct in an office building was measured with a digital anemometer (Testo 405). Readings were taken for both supply and return duct. Readings were also taken at three various depths into the ducts, namely 10 cm, 20 cm and 30 cm. Airflow speeds constantly vary within the ducts. Ten sets of readings were taken for each depth. Mean values were then taken to represent the airflow at a particular depth of a particular duct during a particular time. Measurements were repeated hourly from 8:30am until 4:30pm. It was found that typical airflow speed in the duct in an office building is between 2 and 4  $m \cdot s^{-1}$  as shown in Fig. 4.

III. DESIGN

*A. Vertical Orientation*

The performance of the device depends on the movement of the wing due to the air flow, which is a function of the following parameters and depicted in Fig. 5.

- $\alpha$ : Angle of elevation.
- $h$ : Height of the bluff body.
- $d$ : Distance between the bluff body and the wing.

In addition, the effect of the cross section of the wing on the oscillation of the wing was also investigated.

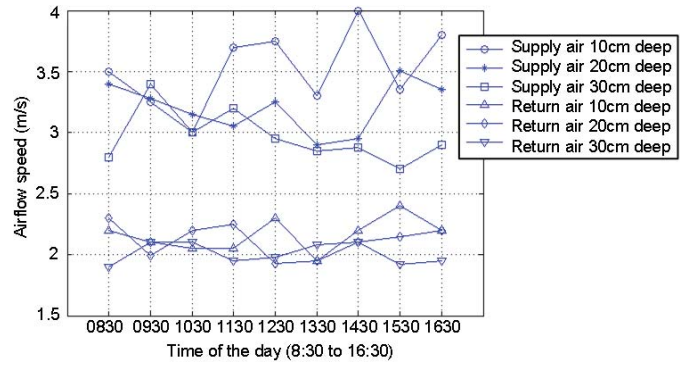


Fig. 4. Airflow speeds measured in the duct in an office building.

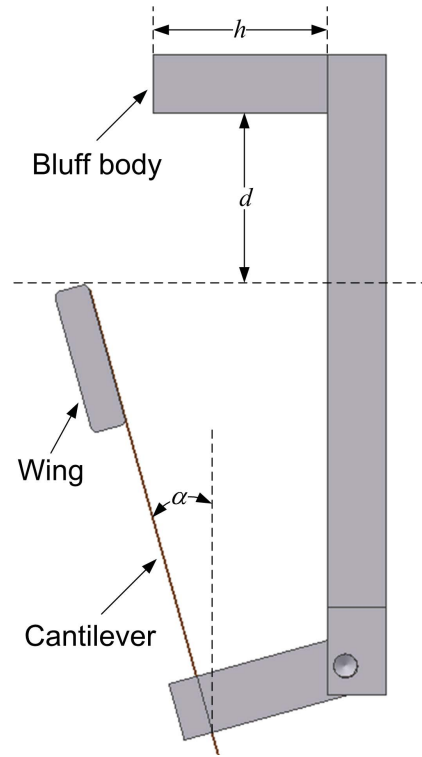


Fig. 5. Schematic view of the device (transducer not included).

The dimensions of the cantilever were 50 mm × 18 mm × 0.2 mm. It was made of beryllium copper. The wing, made of balsa wood, was a rectangular block whose dimensions were 80 mm × 25 mm × 6 mm. The overall mass on the wing was 27.7 grams.

*B. Angle of Elevation*

The angle of elevation was investigated with various combinations of  $h$  and  $d$ .  $h$  was set between 10 and 25 mm and  $d$  between 5 mm and 20 mm. It was found that irrespective of  $h$  and  $d$ , when  $\alpha$  is less than 10° or larger than 20°, the wing did not oscillate. If  $\alpha$  is between 10° and 20°, the minimum airflow speed at which the wing starts oscillating varies from 2  $m \cdot s^{-1}$  to 3  $m \cdot s^{-1}$ . Experimentally, the optimum angle of elevation was found to be 14.5°.

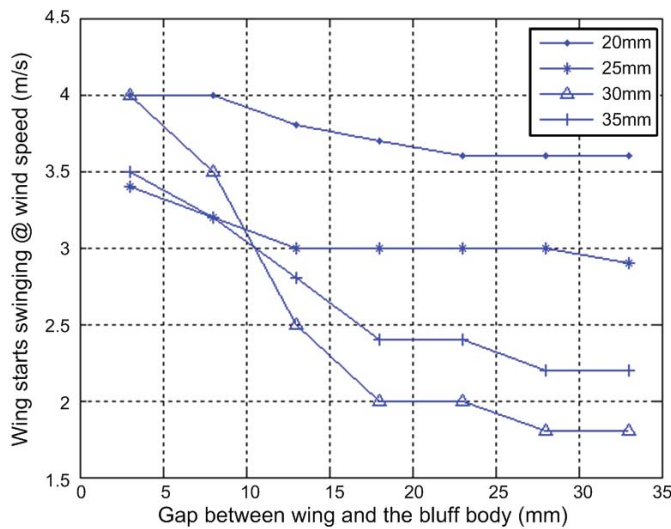


Fig. 6. Comparison of the minimum airflow speed at which the wing starts oscillating with the variation of distance between the wing and the bluff body at different heights (vertical orientation).

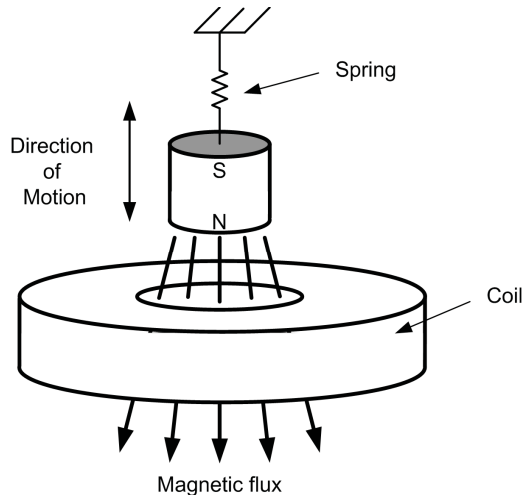


Fig. 7. Electromagnetic transducer for vertical orientation.

### C. Bluff Body

The angle of elevation was set at  $14.5^\circ$  when investigating the effect of the bluff body on the wing. Fig. 6 compares the minimum airflow speeds at which the wing starts oscillating with the variation of distance between the wing and the bluff body at different heights. It was found that, with increasing gap between the bluff body and the wing, the starting airflow speed reduced irrespective of the height of the bluff body. The optimum height of the bluff body was found to be 30 mm. When the bluff body was placed 20 mm (or further) away from the wing, the wing was able to start oscillating at lower airflow speeds.

### D. Electromagnetic Transducer

The electromagnetic transducer used in the vertical device is shown in Fig. 7. A cylinder magnet is attached to the wing at the end of the cantilever spring for the highest displacement. A static coil is placed underneath the magnets. The magnet

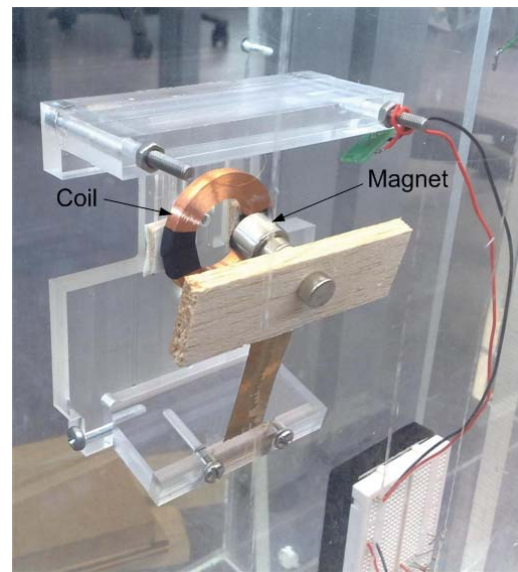


Fig. 8. Final vertical device.

moves up and down with the wing due to the air flow, which causes magnetic flux travelling through the static coil to change, thus an electric current is produced.

### E. Final Device

Fig. 8 is a photograph of the actual device. The cantilever was made of Beryllium Copper (BeCu) and had dimensions of  $50 \text{ mm} \times 18 \text{ mm} \times 0.2 \text{ mm}$ . The cylinder magnet was made of NdFeB-38H. Its diameter was 15 mm and its height was 10 mm. The magnet was fixed 10 mm below the wing and was 7 mm away from the fixed coil. The coil was wound using  $60 \mu\text{m}$  thick copper wire. Its outer and inner diameters were 24 mm and 40 mm, respectively. The thickness is 5 mm. The coil had a static resistance of  $4.7 \text{ k}\Omega$  and approximately 7800 turns. Both the base of the generator and the bluff body were made of acrylic. The overall dimensions of the device were  $12 \text{ cm} \times 8 \text{ cm} \times 6.5 \text{ cm}$ .

### F. Horizontal Orientation

1) *Wing and Bluff Body*: Based on experience in designing the vertical airflow energy harvester, further simulation was conducted using ANSYS fluid-structure interaction analysis to optimize the design of the horizontal airflow energy harvester. Both ANSYS Mechanical and ANSYS CFX tools were used in the simulation. Wings with various cross sections, such as aerofoils and rectangular, have been studied for the optimised design. It was found that the wing with a triangular cross section has the best aerodynamic performance in this application. The operation of this airflow energy harvester is largely dependent on the vertical and horizontal distances between the airfoil and the bluff body,  $a$  and  $b$ , respectively, as well as the elevation angle,  $\alpha$ , as shown in Fig. 9. Tables I to III show the relationship of these variables with the starting airflow speed of the energy harvester. The starting airflow speed here is defined as the airflow speed at which the peak-to-peak movement of the wing is over 3 cm.

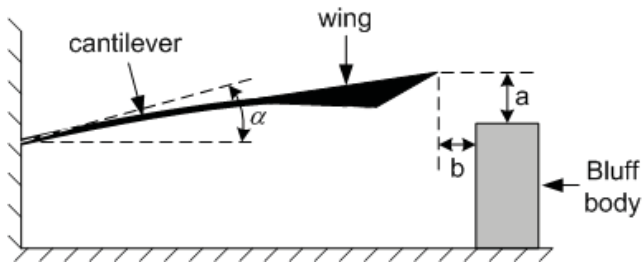


Fig. 9. Optimization of the horizontal airflow energy harvester.

TABLE I

STARTING AIRFLOW SPEED VERSUS VERTICAL DISTANCES BETWEEN THE WING AND BLUFF BODY, a (b = 10 mm, alpha = 30°) IN THE HORIZONTAL ORIENTATION

a (mm)	Airflow Speed (m · s <sup>-1</sup> )
2	5
5	3
8	3
11	5
14	6
17	7
20	8
23	8

TABLE II

STARTING AIRFLOW SPEED VERSUS HORIZONTAL DISTANCES BETWEEN THE WING AND BLUFF BODY, b (a = 8 mm, alpha = 30°) IN THE HORIZONTAL ORIENTATION

a (mm)	Airflow Speed (m · s <sup>-1</sup> )
1	5
4	3
7	3
10	3
13	4
16	5
19	6

Simulation results provided the optimum values for vertical and horizontal distances between the wing and the bluff body, a and b, respectively, as well as the elevation angle, alpha as listed in Table IV.

G. Electromagnetic Transducer

The magnetic circuit of the horizontal energy harvester is shown in Fig. 10. Two mild steel keepers were used to couple the magnetic flux between the top and bottom magnets, which ensured a uniform magnetic field within the air gap. The coil was attached to the base. The four-magnet structure was fixed to a cantilever beam and oscillates with the wing. The magnets moved with respect to the static coil so that the induced current was generated within the coil according to the Faraday’s law. An opening was cut on the wing to allow the coil to fit inside. This magnetic circuit has a better coupling than the one used in the vertical energy harvester. Two sets of magnets were placed

TABLE III

STARTING AIRFLOW SPEED VERSUS ELEVATION ANGLES, alpha (a = 8 mm, b = 10 mm) IN THE HORIZONTAL ORIENTATION

a (mm)	Airflow Speed (m · s <sup>-1</sup> )
5	6
10	5
15	5
20	4
25	4
30	3
35	3
40	5

TABLE IV

OPTIMUM VALUES FROM SIMULATION IN THE HORIZONTAL ORIENTATION

Vertical Distances Between the Airfoil and Bluff Body, a	Horizontal Distances Between the Airfoil and Bluff Body, b	Elevation Angle, alpha
5–8 mm	4–10 mm	30–35°

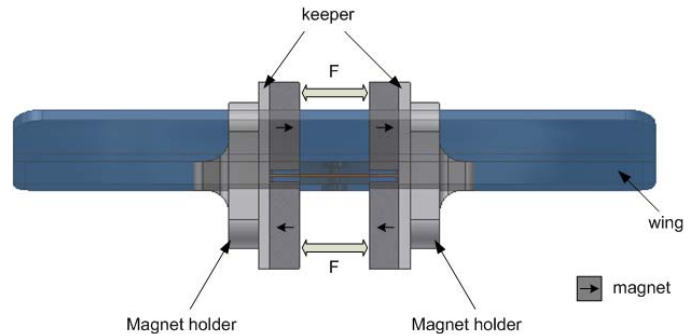


Fig. 10. Electromagnetic transducer for horizontal orientation.

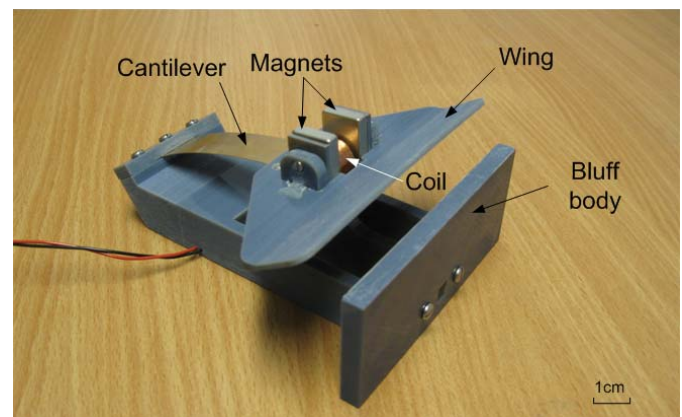


Fig. 11. Horizontal airflow energy harvester.

above and beneath the wing, respectively. This arrangement ensures that attractive forces between upper and lower magnets cancel each other so that the wing will not bend due to the magnetic force.

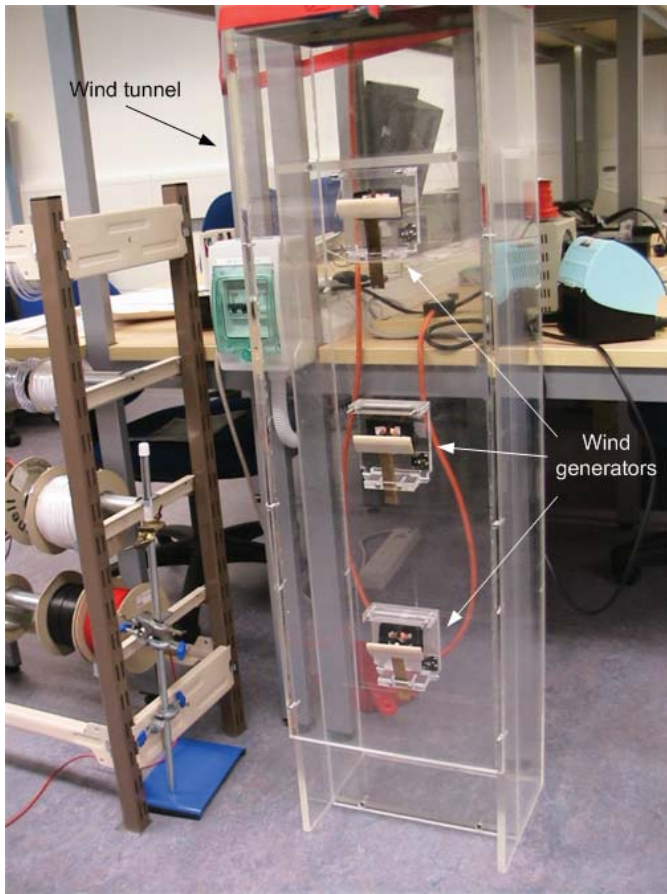


Fig. 12. Vertical energy harvesters in the transparent vertical wind tunnel.

#### H. Final Device

Fig. 11 shows a photo of the airflow energy harvester. The base of the energy harvester and the wing were fabricated using Objet Connex350 multi-material 3D printer. Each component is printed with multiple  $16\ \mu\text{m}$ -thick photopolymer layers. Each photopolymer layer is cured by UV light immediately after it is printed. The material used is sufficiently rigid for this application.

The cantilever is made of  $0.3\ \text{mm}$ -thick BeCu that has good fatigue characteristics. The four magnets are NdFeB to provide strong magnetic field. The coil is wound with  $50\ \mu\text{m}$ -thick copper wire. Its outer and inner diameters are  $15\ \text{mm}$  and  $1\ \text{mm}$ , respectively and it is  $8\ \text{mm}$  thick. The coil has approximately 16000 turns. The total mass of the resonator was measured as  $72.7\ \text{grams}$ . The overall dimensions of the device were  $14.1\ \text{cm} \times 10\ \text{cm} \times 5.5\ \text{cm}$ .

### IV. TEST AND RESULTS

#### A. Vertical Orientation

1) *Test Setup:* Test was done in the wind tunnel as shown in Fig. 12. To generate laminar air flow in the tunnel, a centrifugal fan was used. The wind tunnel had an opening of  $30\ \text{cm} \times 22.5\ \text{cm}$ . The fan can provide the air flow of up to  $10\ \text{m} \cdot \text{s}^{-1}$ . The wall of the wind tunnel was made of acrylic so that oscillation of the generator can be observed in the tests.

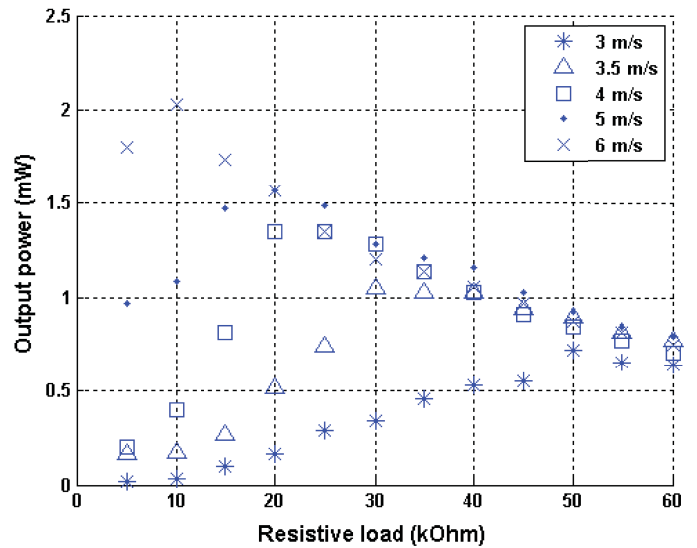


Fig. 13. Output power of the vertical energy harvester versus resistive loads.

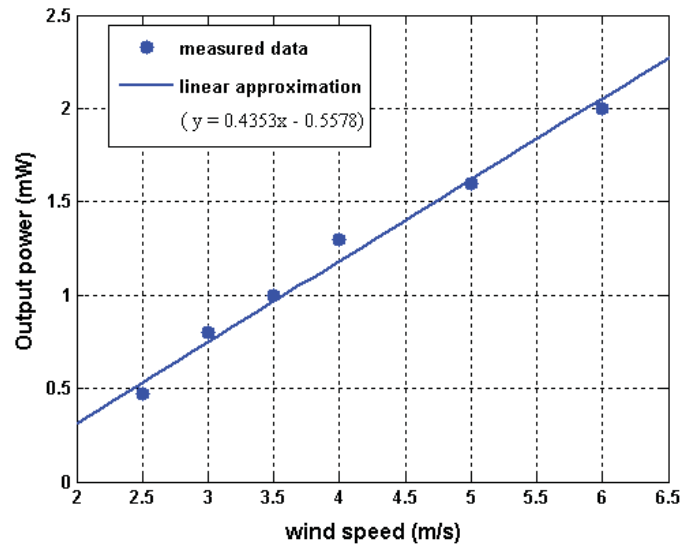


Fig. 14. Output power at the optimum loads of the vertical energy harvester versus airflow speed.

The generator was screwed on a plate, which was placed vertically in the wind tunnel. At each airflow speed, the generator was connected to various resistive loads to find the optimum load and optimum output power.

#### B. Results

Fig. 13 shows the output power of the generator for a variety of resistive loads. It is found that, for increasing airflow speeds, the optimum value of load resistance decreased. This is due to the fact that the stronger the airflow, the larger the force on the wing available to overcome total damping, and so more energy can be extracted for a given displacement. The optimum average output power of the generator with variation of airflow speed is shown in Fig. 14. The generator starts working from an airflow speed of  $2.5\ \text{m} \cdot \text{s}^{-1}$  when it produces an output power of  $470\ \mu\text{W}$ , which is sufficient to power a

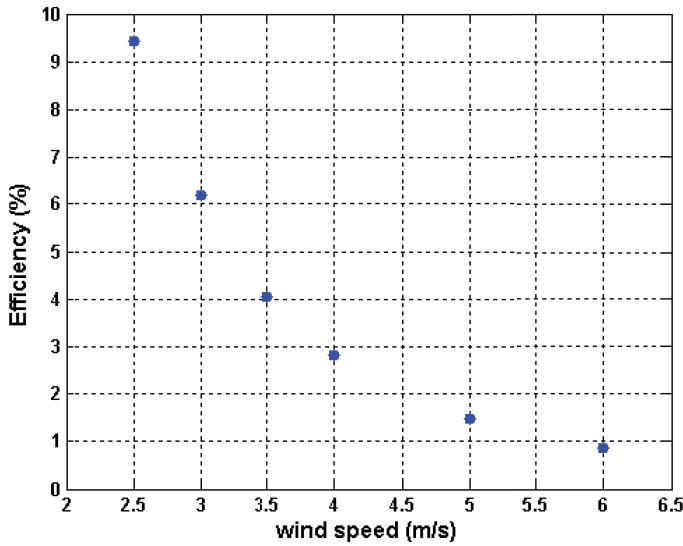


Fig. 15. Efficiency of the vertical energy harvester versus airflow speed.

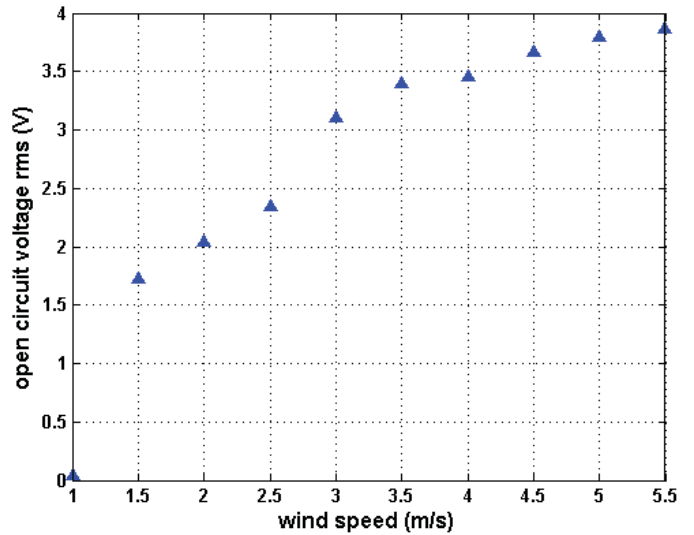


Fig. 17. Open circuit voltage of the horizontal airflow energy harvester.



Fig. 16. Horizontal wind tunnel.

sensor node for periodic sensing and wireless transmission. The output power increases linearly with the airflow speed.

The power available in the airflow,  $P_a$ , is given by:

$$P_a = \frac{1}{2} \cdot \rho \cdot A \cdot v^3 \quad (1)$$

where  $\rho$  is the air density which is  $1.2 \text{ kg/m}^3$  at room temperature and standard atmosphere,  $A$  is the swept area of the wing and  $v$  is the airflow velocity. Dividing power generated by the available power at a certain airflow speed results in the energy transfer efficiency at that airflow speed. Fig. 15 shows the efficiency of the vertical energy harvester. The efficiency reduces with the increasing airflow speed. The reason is that when the wind speed is low, the displacement of the resonator is small. The magnets and the coil are always coupled within such small movement. However, when the wind speed becomes higher, the displacement is so large that the magnets and coil are not always coupled, which reduces the efficiency of the energy harvester.

### C. Horizontal Orientation

1) *Test Setup*: Fig. 16 shows the horizontal wind tunnel used in the test. The wind tunnel had an opening of  $25 \text{ cm} \times 15 \text{ cm}$ . The fan can provide air flow of up to  $10 \text{ m} \cdot \text{s}^{-1}$ .

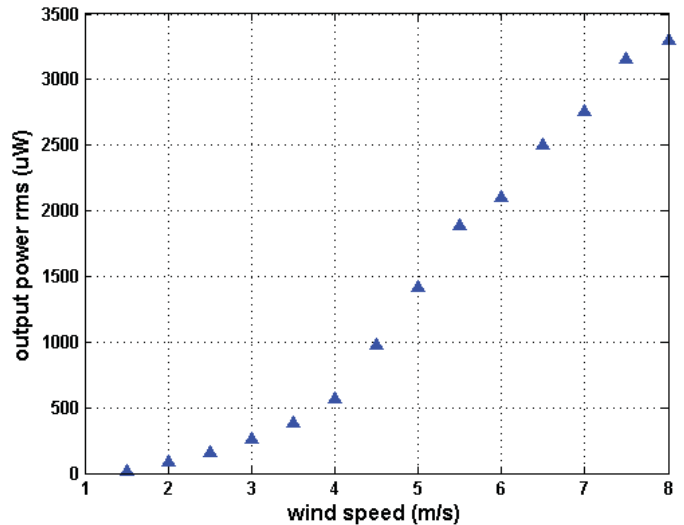


Fig. 18. Output power of the horizontal airflow energy harvester.

A transparent section was attached at the end of the wind tunnel for observing the operation of the airflow energy harvester.

### D. Results

Fig. 17 shows the open circuit voltage of the energy harvester. The open-circuit voltage increases with the airflow speed. When the airflow speed is higher than  $5.5 \text{ m} \cdot \text{s}^{-1}$ , the airflow holds the wing at a certain position because there is no electrical damping and the lift force exceeds the spring force.

Fig. 18 shows that output power also increases with increasing airflow speeds. The energy harvester starts working from an airflow speed of only  $1.5 \text{ m} \cdot \text{s}^{-1}$  when it produces an output power of  $20 \mu\text{W}$ . This start-up airflow speed is lower than that of competing approaches of the same volume. When the airflow speed is between  $2$  and  $4 \text{ m} \cdot \text{s}^{-1}$ , which are typical values measured in the duct in an office building, the output power is between  $90$  and  $573 \mu\text{W}$ , which is sufficient

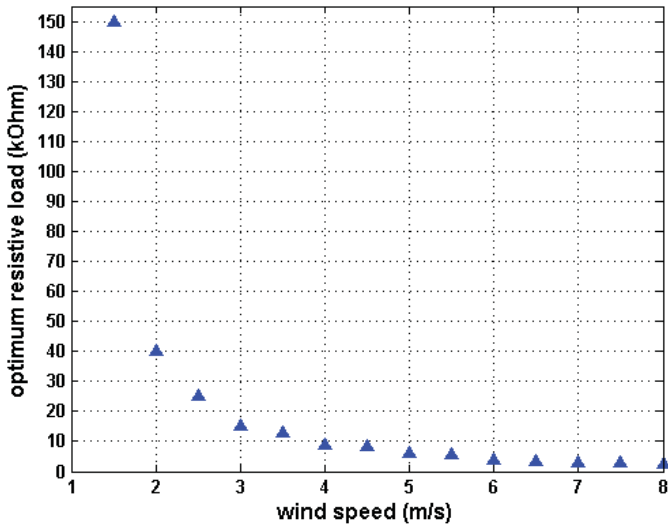


Fig. 19. Optimum resistive load of the horizontal airflow energy harvester.

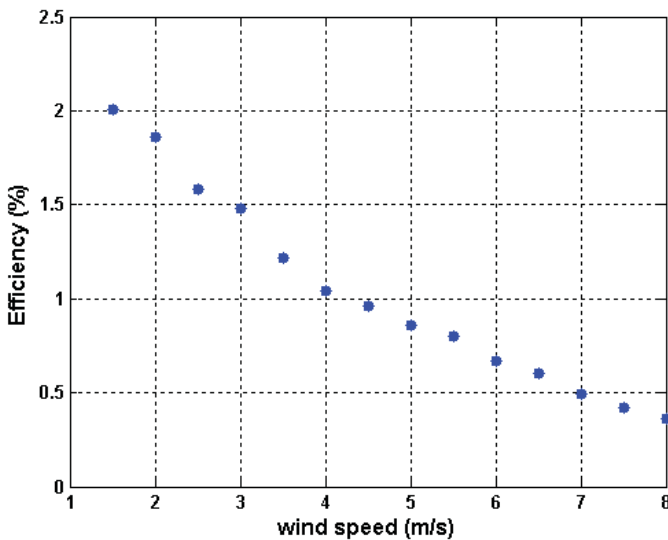


Fig. 20. Efficiency of the horizontal energy harvester versus airflow speed.

for periodic sensing and wireless transmission. Fig. 19 shows that the optimum load resistance reduces with the increase of airflow speed. The reason for this is the same as explained in previous section. Fig. 20 shows the energy transfer efficiency of the horizontal energy harvester. Its efficiency reduces with the increasing airflow speed. The reason is the same as for the device with vertical orientation.

## V. DISCUSSION

### A. Electromagnetic Coupling

Performance of the electromagnetic airflow generator largely depends on the electromagnetic transducer. To achieve the maximum output power, strong electromagnetic coupling is always required. However, if the electromagnetic coupling is too strong, oscillation of the resonator of the airflow generator may be difficult to start. However, if the electromagnetic coupling is weak, the airflow generator cannot produce sufficient power. Therefore, the required degree of electromagnetic

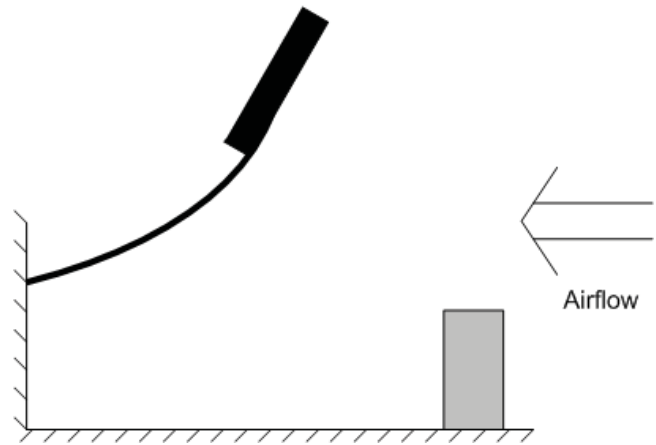


Fig. 21. Stalled wind generator.

coupling depends on the application. In the case of low speed airflow operation, the electromagnetic transducer should not be coupled too well to start with so that the resonator can start oscillating without difficulty and the generator does not extract much enough at the beginning by reducing electrical damping. After momentum is built and stable oscillation is maintained, the transducer can be fully coupled by choosing the optimum electrical load and maximum energy can be extracted. In the case of high airflow speed operation, the electromagnetic coupling should be as strong as possible so that maximum output power can be achieved. Therefore in operation an adaptive load is required to adjust electrical damping depending upon start up conditions and varying airflows.

### B. Limiting Displacement

One potential problem of this type of airflow energy harvester is that when the airflow speed is too high, the airflow force on the wing is much greater than the spring force. The resonator of the generator will stall at a certain position as shown in Fig. 21. If this happens too frequently, the cantilever of the energy harvester can be damaged due to excessive stress and its lifetime can be significantly reduced. Therefore, it is important to limit the displacement of the resonator. A possible method to limit its displacement is to use the adaptive load to control the displacement by varying the electrical damping. When the airflow speed is high, the electrical damping should be increased by reducing the electrical load to prevent stalling from happening. When the airflow speed is reduced, the electrical load can be adjusted back to the optimum value. An electrical load selection system is required to achieve this function. Alternatively, mechanical stops can be used to physically limit the displacement of the resonator. However, the impact between the resonator and the mechanical stops can cause failure in the cantilever of components on the wing, which can potentially reduce the life time of the energy harvester.

### C. Comparisons With Other Devices

Fig. 22 compares output power of various wind/airflow energy harvesters mentioned in Section I and the two devices

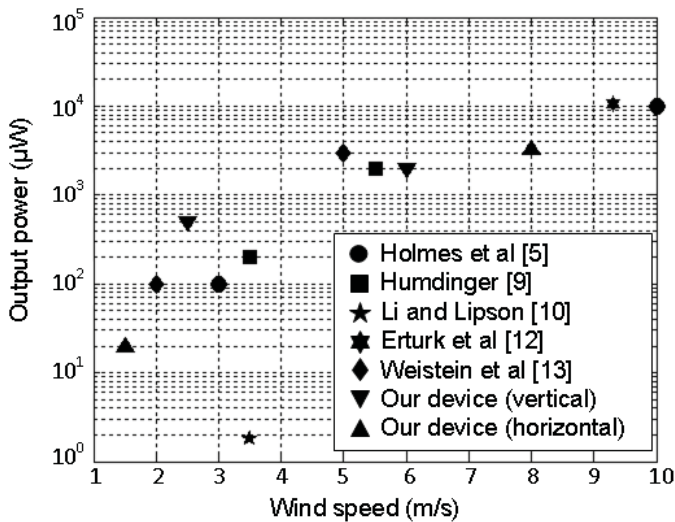


Fig. 22. Comparisons of output power of various wind/airflow energy harvesters.

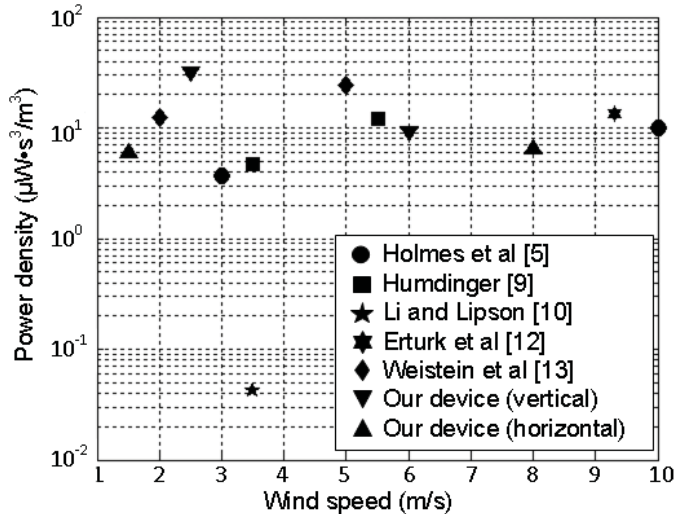


Fig. 23. Comparisons of power density of various wind/airflow energy harvesters.

presented in this paper. It is found that the horizontal energy harvester presented in this paper has the lowest operation wind speed (1.5 m/s).

Fig. 23 compares power density of various wind/airflow energy harvesters mentioned in Section I and the two devices presented in this paper. As the output power is proportional to the cubic of the wind speed, the power density was calculated by dividing output power by the cubic of its corresponding wind speed. It is found that the vertical energy harvester presented in this paper has the highest power density when it is operated at 2.5 m/s.

## VI. CONCLUSION

This paper describes a novel type of flapping electromagnetic airflow energy harvesters. Two orientations of such energy harvesters were studied, i.e. vertical and horizontal. Due to gravity, the initial displacement of the mass is different when the device is placed vertically and horizontally. The elevation angle as well as size and position of the bluff body

were found to be different in the two cases. These values need to be reconfigured according to the particular application.

Experimentally, it was found that the vertical airflow energy harvester has the highest power density among wind energy harvesters reported in the literatures so far and the improved horizontal airflow energy harvester has the lowest starting airflow speed of only  $1.5 \text{ m} \cdot \text{s}^{-1}$  and produced a minimum output power of  $90 \text{ } \mu\text{W}$  at the airflow of  $2 \text{ m} \cdot \text{s}^{-1}$  and above. This amount of power is sufficient for powering wireless sensor nodes in HVAC systems in buildings.

For the oscillating airflow generator, one major drawback is that there is no mechanism to limit the displacement of the tip mass. If the airflow speed becomes high ( $> 10 \text{ m} \cdot \text{s}^{-1}$ ), the displacement of the mass can be very large, which may reduce the lifespan of the device. One potential solution is to control the electrical damping by varying the electrical load. To achieve this, the transducer must have high coupling. However, if the electromagnetic coupling is too high, the generator may not work at low airflow speed. There is thus a tradeoff between degree of electromagnetic coupling and minimum working airflow speed. Further investigation will be done to find a suitable transducer to enable damping control to limit the mass displacement while not increasing the minimum starting airflow speed.

## REFERENCES

- [1] D. Snoonian, "Smart buildings," *IEEE Spectr.*, vol. 40, no. 8, pp. 18–23, Jun. 2003.
- [2] D. M. Rowe, "Thermoelectric waste heat recovery as a renewable energy source," *Int. J. Innov. Energy Syst. Power*, vol. 1, no. 1, pp. 13–23, 2006.
- [3] S. P. Beeby, M. J. Tudor, and N. M. White, "Energy harvesting vibration sources for microsystems applications," *Meas. Sci. Technol.*, vol. 17, no. 12, pp. 175–195, Oct. 2006.
- [4] G. M. J. Herberta, S. Iniyamb, E. Sreevalsanc, and S. Rajapandian, "A review of wind energy technologies," *Renew. Sustain. Energy Rev.*, vol. 11, no. 6 pp. 1117–1145, Aug. 2007.
- [5] A. S. Holmes, G. Hong, K. R. Pullen, and K. R. Buffard, "Axial-flow microturbine with electromagnetic generator: Design, CFD simulation and prototype demonstration," in *Proc. 17th IEEE Int. Conf. Micro Electro Mech. Syst.*, May 2004, pp. 568–571.
- [6] A. S. Holmes, D. A. Howey, A. Bansal, and D. C. Yates, "Self-powered wireless sensor for duct monitoring," in *Proc. Power Micro Electro Mech. Syst.*, 2010, pp. 115–118.
- [7] S. Priya, C.-T. Chen, D. Fye, and J. Zahnd, "Piezoelectric windmill: A novel solution to remote sensing," *Jpn. J. Appl. Phys.*, vol. 44, no. 3, pp. 104–107, 2005.
- [8] P. D. Mitcheson, E. M. Yeatman, G. K. Rao, A. S. Holmes, and T. C. Green, "Energy harvesting from human and machine motion for wireless electronic devices," *Proc. IEEE*, vol. 96, no. 9, pp. 1457–1486, Sep. 2008.
- [9] Humdinger Wind Energy. (2010, Jul. 28) [Online]. Available: <http://www.humdingerwind.com>
- [10] S. Li and H. Lipson, "Vertical-stalk flapping-leaf generator for parallel wind energy harvesting," in *Proc. ASME/AIAA Conf. Smart Mater., Adapt. Struct. Intell. Syst.*, vol. 2, 2009, pp. 611–619.
- [11] L. Tang, M. P. Paidoussis, and J. Jiang, "Cantilevered flexible plates in axial flow: Energy transfer and the concept of flutter-mill," *J. Sound Vibrat.*, vol. 326, nos. 1–2, pp. 263–276, Sep. 2009.
- [12] A. Erturk, W. G. R. Vieira, C. De Marqui, and D. J. Inman, "On the energy harvesting potential of piezoaeroelastic systems," *Appl. Phys. Lett.*, vol. 96, no. 18, pp. 184103-1–184103-3, May 2010.
- [13] L. A. Weinstein, M. R. Cacan, P. M. Soand, and P. K. Wright, "Vortex shedding induced energy harvesting from piezoelectric materials in heating, ventilation and air conditioning flows," *Smart Mater. Struct.*, vol. 21, no. 4, pp. 045003-1–045003-10, Mar. 2012.

**Dibin Zhu** received the B.Eng. degree in information and control engineering from Shanghai Jiao Tong University, Shanghai, China, in 2004, the M.Sc. degree in RF communication systems and the Ph.D. degree in electrical and electronic engineering from the University of Southampton, Southampton, U.K., in 2005 and 2009, respectively. His Ph.D. research was on the topic of methods of frequency tuning vibration based micro-generators.

He joined the University of Southampton, Southampton, U.K., in 2004, where he is currently a Research Fellow with the Electronics and Electrical Engineering Group, School of Electronics and Computer Science. He has contributed to multiple research projects on energy harvesting, including the most recent one on the development of technology building blocks for structural health monitoring sensing devices in aeronautics (TRIAD), which is funded under EU FP7. His current research interests include energy harvesting from various sources, vibration, wind, human movement, and their applications.

**Steve P. Beeby** received the Ph.D. degree in micromechanical resonators from the University of Southampton, Southampton, U.K., in 1998.

He is currently a Professor with the School of Electronics and Computer Science, University of Southampton. He is the coordinator of a European Union Framework Integrated Project "MicroFIEX" and is a Principal or Co-Investigator on three additional projects. He has co-authored one book, entitled *MEMS Mechanical Sensors*, more than 220 publications, and holds five patents. His current research interests include energy harvesting, MEMS, active printed materials development, and biometrics.

Dr. Beeby was awarded a prestigious EPSRC Advanced Research Fellowship in 2001 to investigate the combination of screen-printed piezoelectric materials with micromachined structures. He is a Co-Founder of Perpetuum Ltd., a university spin-off company based on vibration energy harvesting, formed in 2004.

**Michael J. Tudor** received the B.Sc. (Eng.) degree in electronic and electrical engineering from University College London, London, U.K., and the Ph.D. degree in physics from Surrey University, Guildford, U.K.

He joined Schlumberger Industries in 1987, working first at their Transducer Division in Farnborough and then at their Research Centre in Paris, France. He joined the University of Southampton, Southampton, U.K., in 1990, as a Lecturer with research interests in optical fiber sensors and micromachined sensors. He moved to ERA Technology in 1994, where he became the Microsystems Program Manager. He returned to the School of Electronics and Computer Science, University of Southampton, in 2001 to pursue university based research in microsystems. He is currently a Principal Research Fellow. He has authored or co-authored more than 110 publications and is both a Chartered Physicist and Engineer.

**Neil M. White** (M'01–SM'02) received the Ph.D. degree from the University of Southampton, Southampton, U.K., in 1988, for a thesis describing the piezoresistive effect in thick-film resistors.

He is the Head of the Electronic Systems and Devices (ESD) Group and Deputy Head of School (Enterprise). He was appointed as a Lecturer within the School in 1990 and promoted to Senior Lecturer in 1999, Reader in 2000, and was awarded a Personal Chair in 2002. He lectures on digital electronics, electronic measurement techniques, and advanced instrumentation and sensors. He has co-authored *Intelligent Sensor Systems* (Institute of Physics Publishing, 1994), *MEMS: Mechanical Sensors* (Artech House), and more than 200 scientific papers in the area of sensors and instrumentation systems. He holds ten patents. His current research interests include thick-film sensors, intelligent instrumentation, MEMS, self-powered microsensors, and sensor networks.

Prof. White was a recipient of the 2009 Calendar Silver Medal, awarded by the Institute of Measurement and Control for his outstanding contribution to the art of instruments and measurement. He is a Chartered Engineer, fellow of the IET, fellow of the IoP, and a Chartered Physicist. He was the Chairman of the Instrument Science and Technology Group of the IoP from 1997 to 1999. He is a member of the Peer Review College for the EPSRC and is on the editorial board of the international journals *Sensor Review* and the *Journal of Materials Science: Materials in Electronics*. He is also a Series Editor for the *Integrated Microsystems* series (Artech House). He is a former Director and Co-Founder of the university spin-out company Perpetuum Ltd., which specializes in vibration energy harvesting.

**Nick R. Harris** received the Ph.D. degree from the Department of Mechanical Engineering, University of Southampton, Southampton, U.K., in 1997.

He is a Senior Lecturer with the School of Electronics and Computer Science, University of Southampton. He was a Principal Engineer with Era Technology, Microsystems and Materials Group, in 1998, before returning to the University of Southampton as a Senior Research Fellow, with research interests in miniaturized fluidic systems resulting in a unique type of microfluidic particle concentrator using ultrasonic standing waves. He has authored or co-authored more than 180 publications in the fields of wireless sensor networks, biosensors, microfluidic systems, and processing. His current research interests include self-powered health and usage monitors and embedded condition-monitoring microsystems, wireless sensor networks and analogue, and digital electronic sensor circuit design.

Dr. Harris is a member of the IET and a Chartered Engineer, and a Co-Founder of Perpetuum Ltd., an energy-harvesting spin-off company from Southampton.